2013 International Nuclear Atlantic Conference - INAC 2013
Recife. PE. Brazil. November 24-29. 2013
ASSOCIAÇÃO BRASILEIRA DE ENERGIA NUCLEAR - ABEN
***ISBN:* 978-85-99141-05-2**

NEUTRONIC CHARACTERIZATION OF CYLINDRICAL CORE OF MINOR EXCESS REACTIVITY IN THE NUCLEAR REACTOR IPEN/MB-01 FROM THE MEASURE OF NEUTRON FLUX DISTRIBUTION AND ITS REACTIVITY RATIO

Ulysses d´Utra Bitelli[1], Vitor O. G. Arêdes[1], Luiz E. C. Mura[1], Diogo F. dos Santos[1], Alexandre P. da Silva[1]

[1] Instituto de Pesquisas Energéticas e Nucleares (IPEN / CNEN - SP)
Av. Professor Lineu Prestes 2242
05508-00 São Paulo, SP
ubitelli@ipen.br
vitoraredes@ipen.br

ABSTRACT

When compared to a rectangular parallelepiped configuration the cylindrical configuration of a nuclear reactor core has a better neutron economy because in this configuration the probability of the neutron leakage is smaller, causing an increase in overall reactivity in the system to the same amount of fuel used. In this work we obtained a critical cylindrical configuration with the control rods 89.50% withdraw from the active region of the IPEN/MB-01 core. This is the cylindrical configuration minimum possible excess of reactivity. Thus we obtained a cylindrical configuration with a diameter of only 28 fuel rods with lowest possible excess of reactivity. For this purpose, 112 peripheral fuel rods are removed from standard reactor core (rectangular parallelepiped of 28x28 fuel rods). In this configuration the excesses of reactivity is approximated 279 pcm. From there, we characterize the neutron field by measuring the spatial distribution of the thermal and epithermal neutron flux for the reactor operating power of 83 watts measured by neutron noise analysis technique and 92.08 ± 0.07 watts measured by activation technique [10]. The values of thermal and epithermal neutron flux in different directions, axial, radial north-south and radial east-west, are obtained in the asymptotic region of the reactor core, away from the disturbances caused by the reflector and control bar, by irradiating thin gold foils infinitely diluted (1% Au - 99% Al) with and without (bare) cadmium cover. In addition to the distribution of neutron flux, the moderator temperature coefficient, the void coefficient, calibration of the control rods were measured.

1. INTRODUCTION

The cylindrical core reactor has geometry more effective when compared to a rectangular parallelepiped shape, because in cylindrical the probability of leakage is smaller, causing an increase in overall system reactivity.

Thus if we use all the fuel rods from the default rectangular setting of the reactor IPEN \ MB-01, to get a new cylindrical configuration with 680 fuel rods, we have to insert control rods, because this configuration has an excess reactivity of 3271 pcm, 814 pcm more than the standard rectangular configuration, causing greater distortion in neutron flux, both internally and externally where are the nuclear channels. In this work, we want to obtain a cylindrical configuration with the lowest excess reactivity possible by removing a certain amount of fuel

***ISBN:* 978-85-99141-05-2**

rods out into the cylinder. From procurement of cylindrical configuration desired, the neutron field was characterized by measuring the spatial and energetic distributions [8].

The calculation methodology currently used to obtain values of neutron flux for different core configurations are performed by the program MCNP-4C, using its associated nuclear data libraries such as ENDF-B.VIII and JENDL [5]. The calculated values are compared with experimental results and can be used as an additional data set for comparison to the Reactor Physics community to validate its calculation methodologies and associated nuclear data libraries.

The values of thermal neutron flux and epithermal are obtained experimentally by irradiating gold foil naked and covered with cadmium and measure the nuclear reaction rate of radioactive induced in these activation detectors irradiated in a certain position in the reactor core.

The objective of this work is to obtain experimental values of the curvature of the neutron flux in the axial direction, radial north-south and radial east-west, into the asymptotic region of the reactor core in its cylindrical core configuration, away from the disturbances caused by reflector and control bar. The extension of the asymptotic region can be determined from the measurement of the ratio of cadmium in foils of activation.

All results will be compared with experimental values obtained from the calculation using the program MCNP-4C with its associated nuclear data libraries.

2. METHODOLOGY

The cylindrical configuration of lower excess of reactivity found by removal of fuel rods, in order to reduce the diameter of the reactor core, has a diameter of 28 fuel rods, e.g. Fig. 1. The excess of reactivity of this new configuration is approximately eight (8) times smaller than the default 28x26 rectangular, approximately 2457 pcm for standard configuration, and approximately 279 pcm for the new cylindrical configuration.

For the experiments irradiation and counting of foils, we had activation foils infinitely dilute of gold-aluminum (Au-Al), with a percentage of gold in the alloy of 1.0%, which makes it unnecessary the self-shielding adjust of the neutron flux. We also used high purity foils of gold (Au197) scandium (SC45), titanium (Ti47), Nickel (Ni58), indium (In115). Table 1 shows the characteristics of the activation foils.

The activation foils are fixed to a board of Lucite, e.g. Fig. 2 and 3, inserted between the channels of the reactor core (spaces between the fuel rods). The irradiation time was estimated by the half-life of the radionuclide formed in the nuclear reaction of interest and the activation cross section of the target irradiated. In some cases the foils used were covered with cadmium aiming to avoid interference from thermal neutrons. All irradiations were conducted at (92.08±0.07) watts of power measured by foil activation technique.

2013 International Nuclear Atlantic Conference - INAC 2013
Recife. PE. Brazil. November 24-29. 2013
ASSOCIAÇÃO BRASILEIRA DE ENERGIA NUCLEAR - ABEN
***ISBN:* 978-85-99141-05-2**

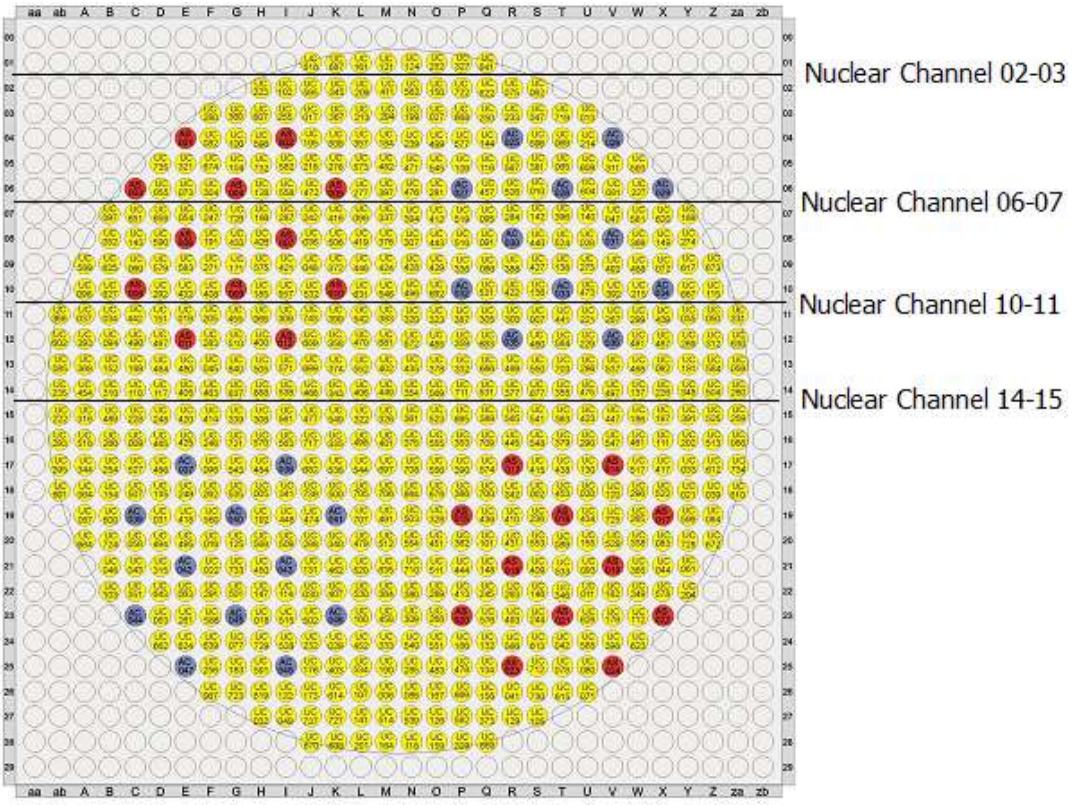

Figure 1: Cylindrical Configuration of the minor excess of Reactivity (28x28 fuel rods) of the IPEN/MB-01 Reactor.

Table 1: Characteristics of the activation foils (detectors).

Irradiated Foil	Nuclear Reaction /Product	Product Half-life	Mass (g)	Thickness (cm)	Irradiation time
1%Au-99%Al *	$Au^{197}(n,\gamma)Au^{198}$	64.56 h	0.025	0.02	1 h
1%Au-99%Al	$Au^{197}(n,\gamma)Au^{198}$	64.56 h	0.025	0.02	1 h
100%Au	$Au^{197}(n,\gamma)Au^{198}$	64.56 h	0.01	0.001	1 h
100%Au *	$Au^{197}(n,\gamma)Au^{198}$	64.56 h	0.01	0.001	1 h
Sc	$Sc^{45}(n,\gamma)Sc^{46}$	2011.92 h	0.0169	0.00127	1 h
Sc *	$Sc^{45}(n,\gamma)Sc^{46}$	2011.92 h	0.0176	0.00127	1 h
Ti	$Ti^{47}(n,p)Sc^{47}$	44 h	0,05	0.00254	3 h
Ni	$Ni^{58}(n,n)Co^{58m}$	1728 h	0.1	0.00254	2 h
In	$In^{115}(n,n')In^{115m}$	4.5 h	0.039	0.00127	1 h
In *	$In^{115}(n,n')In^{115m}$	4.5 h	0.039	0.00127	1 h

* cadmium box: 0.5 mm thickness

2013 International Nuclear Atlantic Conference - INAC 2013
Recife. PE. Brazil. November 24-29. 2013
ASSOCIAÇÃO BRASILEIRA DE ENERGIA NUCLEAR - ABEN
***ISBN:* 978-85-99141-05-2**

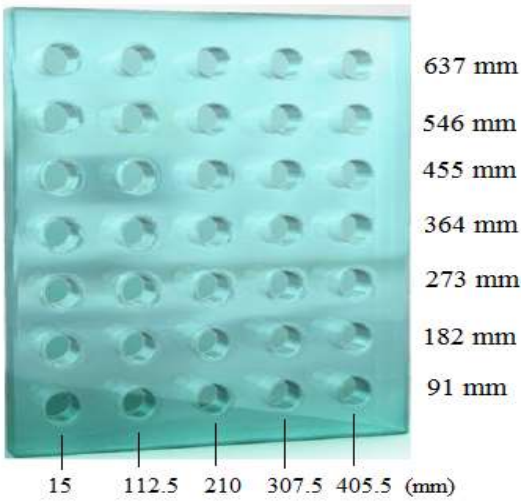

Figure 2: Illustration of lucite board and the fittings for activation detector.

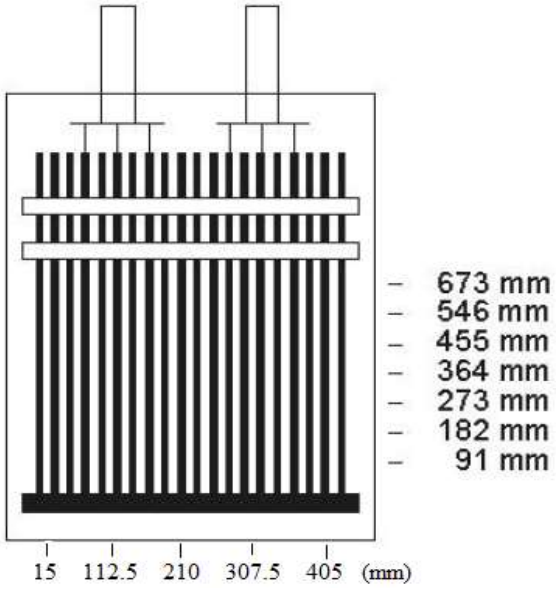

Figure 3: Illustration of the dimensions of lucite board relative to the reactor core.

The high purity gold foils and infinitely diluted were irradiated in various positions of four nuclear channels, e.g. Fig. 1, with and without cadmium coverage for mapping the neutron flux.

To characterize the energy spectrum of this reactor core configuration, we used different materials that work in different energy level, which were irradiated in the central position of the reactor core in the channel 14-15. Tables 2, 3 and 4 show the activation characteristics of the detectors used to obtain the spectrum of neutrons.

***ISBN:* 978-85-99141-05-2**

Table 2: Nuclear Reactions and response range of the thermal activation detectors.

Foil	Nuclear Reaction	Action Range (Mev)
Sc	$Sc^{45}(n, \gamma)Sc^{46}$	1.0×10^{-9}___1.3×10^{-6}
Au	$Au^{197}(n, \gamma)Au^{198}$	1.0×10^{-8}___6.3×10^{-6}

* 90% of Nuclear reaction rate.

Table 3: Nuclear Reactions and response range of the intermediates activation detector .

Foil	Nuclear Reaction	Action Range (Mev)
Sc	$Sc^{45}(n, \gamma)Sc^{46}$ **	2.5×10^{-7}___4.5×10^{-3}
Au	$Au^{197}(n, \gamma)Au^{198}$ **	2.8×10^{-6}___3.0×10^{-5}

* 90% da of Nuclear reaction rate.
** Irradiation foils with coverage of cadmium.

Table 4: Nuclear Reactions and response range of the fast activation detector .

Foil	Nuclear Reaction	Action Range (Mev)
In	In^{115} (n,n') In^{115m}	1.0___6.7
In	In^{115} (n,n') In^{115m} **	1.0___6.7
Ni	Ni^{58} (n,p) Co58	1.8___8.2
Ti	Ti^{47} (n,p) Sc^{47}	1.8___8.2

* 90% da of Nuclear reaction rate.
** Irradiation foils with coverage of cadmium.

The integrals counts of gamma photo peak of the radionuclide were performed by a high purity germanium detector, using the MAESTRO software installed on a computer (PC). Using the ORIGIN, exponential adjustments were made from three decay counts of 20mins for each position and various counts in the central region of the core (statistically better), so as to obtain the activity value at the end of irradiation (A_0), as shown in figure 4, and thereby its saturation activity (nuclear reaction rate at the place of irradiation).

2013 International Nuclear Atlantic Conference - INAC 2013
Recife. PE. Brazil. November 24-29. 2013
ASSOCIAÇÃO BRASILEIRA DE ENERGIA NUCLEAR - ABEN
***ISBN:* 978-85-99141-05-2**

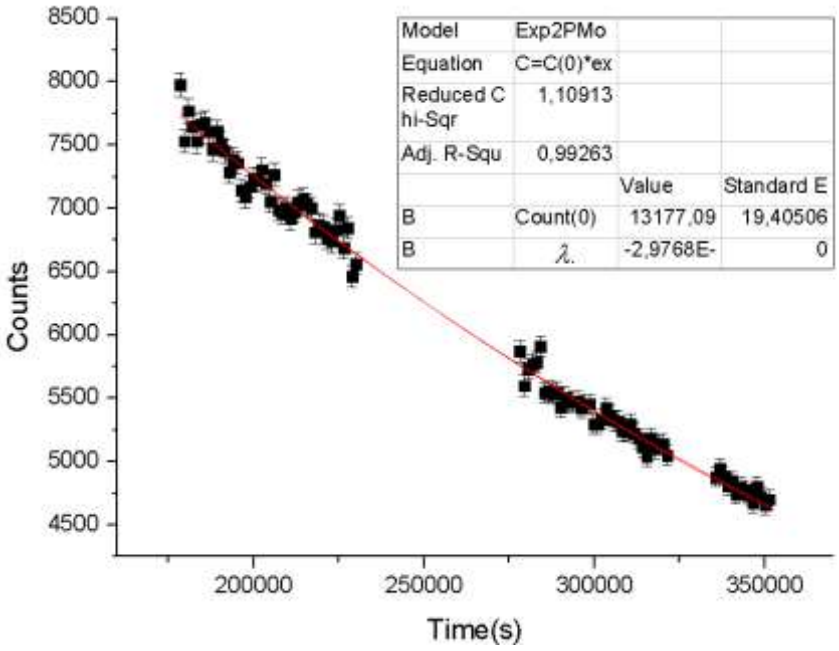

Figure 4: Exponential adjustment decay curve of the photo peak counts for the central position of the reactor core.

After found the flux at the positions of interest, curves of the thermal neutron flux (energy below 0.55 eV) and epithermal (energy above 0.55 eV) were plotted throughout the reactor core in the axial and radial regions. The saturation activities were also used as input to the software SAND-BP to calculate the neutron spectrum.

3. THEORY

Neutrons have no electrical charge, so they are detected indirectly [6]. The technique of activation analysis is frequently used to detect them. For this work, were used detectors called activation foils composed of 1% of gold (*Au*) and 99% of aluminum (*Al*), called infinitely diluted foil [2]. There is also high purity foils, which provide a higher nuclear activity constituted by 100% of the target nucleus, but has the inconvenience of needing to make corrections in the calculations because of the phenomena of disturbance of neutron flux.

The reaction that occurs at Au because of the neutronic field is radioactive capture, ^{197}Au (n, γ) ^{198}Au, the target nucleus captures a neutron and emits a gamma ray of approximately 411.80 keV with a high probability emission of 95.56% . The activation foils were irradiated in a reactor critical, but until achieve the desired power the foils are irradiated by neutronic field. Thus, it is necessary to correct this addition of activity due to the rise of the ramp of power, it is of interest only the activity induced in the foils because of the neutron flux for stable power [2]. The ramp factor F_R can be determined by equation (1),

2013 International Nuclear Atlantic Conference - INAC 2013
Recife. PE. Brazil. November 24-29. 2013
ASSOCIAÇÃO BRASILEIRA DE ENERGIA NUCLEAR - ABEN
***ISBN:* 978-85-99141-05-2**

$$F_R = \frac{1}{1+\frac{T}{t}} \tag{1}$$

the period T is given by equation (2),

$$T = \frac{T_R}{\ln\left(\frac{P}{P_0}\right)} \tag{2}$$

where P is the final power of irradiation, P_0 is the initial power and T_R the time of ramp rise, timed from P_0 to P, as illustrated in Figure 1.

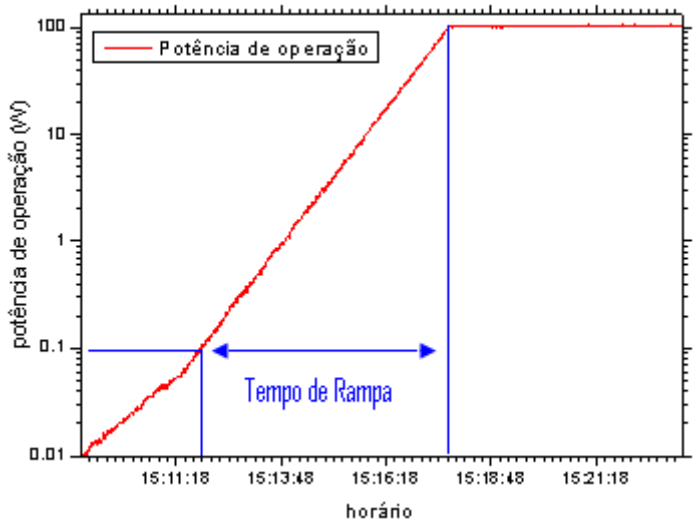

Figure 1: The power level as a function of time.

After irradiation of activation foils, waited a few minutes to decay 95% of the main fission products then these leaves were analyzed through an Ortec HPGe detector centered at the photo peak of energy 411.80 keV for the gold *(Au*). Thus were obtained the photo peak areas that are counts (net) as disintegrations per second.

The nuclear reaction rate is equal to the saturation activity which can be obtained when a detector is irradiated for an infinite time, much longer than its half-life, making impracticable the achievement of experimental saturation activity. Even if the activation foils were irradiated for a very long time, it would be impossible to take them immediately to the HPGe detector [7]. The activity of saturation on the basis of counts obtained in the detector is given by equation (3).

$$A^{\infty} = \frac{\lambda . net . e^{\lambda t_e}}{\varepsilon . I . \left(1 - e^{-\lambda t_i}\right) . \left(1 - e^{-\lambda t_c}\right)} = \frac{\lambda . A_0}{\varepsilon . I . \left(1 - e^{-\lambda t_i}\right) . \left(1 - e^{-\lambda t_c}\right)} \tag{3}$$

where:

***ISBN:* 978-85-99141-05-2**

λ is the decay constant of the radioisotope formed;
net is the photo peak area or count;
A_0 is the initial activity;
te is the waiting time between the end of irradiation and counting;
ti is the irradiation time;
tc is the counting time;
I is the Branching rate;
ε is the efficiency counting (HPGe).

The efficiencies ε of the HPGe detector were determined by counts of radioactive source of ^{152}Eu that had an initial activity on 01/03/1991 A_0=13.30 ± 0.29 KBq with a statistical confidence of 2σ. The counting efficiency is given by equation (4),

$$\varepsilon = \frac{net}{LT.I.A} \tag{4}$$

where:
LT (Live Time) is the counting time discounting the "dead time" of the detector;
A is the activity of 152Eu at the time of counting.

With only two counts is possible to determine the decay curve of each position and get its initial activity A_0 by equation (5) and its activity Saturation A^{∞} (3) as shown in the figure 2. In this case more counts improve the adjustment in the decay curve and closer to the physical reality will be the value obtained for A_0.

$$A = A_0.e^{-\lambda.t_e} \tag{5}$$

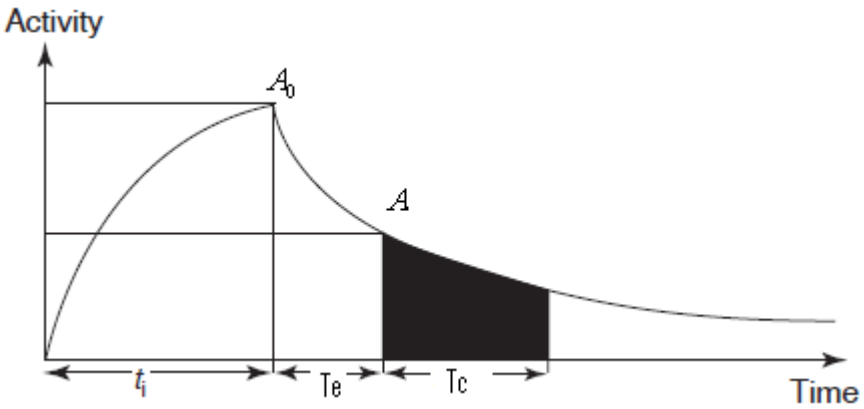

Figure 2: Variation of the activity of the detector as a function of time.

The activation detector is not only sensitive to a specific range of the neutronic spectrum. Thus, is necessary to discriminate the parcel of the neutron energy of interest. The induced saturation activity in bare gold foil is due to thermal neutrons and intermediates, equation (6), the parcel of fast neutrons is insignificant because of their low cross-section for energies above 1.05 MeV , these foils are transparent to fast neutrons [1].

***ISBN:* 978-85-99141-05-2**

$$A^{\infty}_{nua} = A^{\infty}_{ter} . A^{\infty}_{\text{int}} \tag{6}$$

For the amount related the saturation activity of intermediate flux in a foil is necessary to cover it with a small box of cadmium. Cadmium (Cd) is not a perfect filter because it does not absorbs only thermal neutrons but also intermediate neutrons and the cadmium-correction factor fix this problem, equation (7).

$$A^{\infty}_{\text{int}} = F_{cd} . A^{\infty}_{cd} \tag{7}$$

This factor is tabulated in literature and depends on the thickness of cadmium and the material, or may be obtained by the Monte Carlo method [5], equation (8),

$$F_{cd} = \frac{A^{\infty}_{epi}}{A^{\infty}_{cd}} \tag{8}$$

where:
A^{∞}_{epi} is the saturation activity for neutrons with energy between the spectrum thermal and intermediate in a bare activation detector and A^{∞}_{cd} is the saturation activity for detector covered with cadmium above the Thermal energy.

The ratio of cadmium to the point where it is performing the measurement for infinitely diluted foil is given by equation (9).

$$R_{cd} = \frac{A^{\infty}_{nua}}{A^{\infty}_{cd}} \tag{9}$$

Thus, the thermal saturation activity can be obtained by equation (6) or (10).

$$A^{\infty}_{ter} = A^{\infty}_{nua} . \left(1 - \frac{F_{cd}}{R_{cd}}\right) \tag{10}$$

As $A^{\infty} = \Sigma_{act} V \varphi$ where Σ_{act} is the average activation macroscopic cross section and V the volume of the detector. The thermal neutron flux is given by equation (11).

$$\varphi_{ter} = \frac{A^{\infty}_{ter} . P_a}{N_a . m . \sigma_{atv} . G_{ter}} \tag{11}$$

where:
P_a is the atomic weight of the target nucleus;
N_a is the Avogadro's number;
m is the mass of the activation detector ;
σ_{atv} is the average microscopic cross section;
G_{ter} disturbance factor in the thermal flux.

The term G is introduced into the equation to restore the neutron flux and can be ignored in infinitely diluted foil (*Au-Al*) where the target is diluted [6]. For high purity activation foils,

2013 International Nuclear Atlantic Conference - INAC 2013
Recife. PE. Brazil. November 24-29. 2013
ASSOCIAÇÃO BRASILEIRA DE ENERGIA NUCLEAR - ABEN
***ISBN:* 978-85-99141-05-2**

the disturbance factor *G* was found experimentally with the irradiation of gold foil in different concentrations in the same positions in the core of the nuclear reactor, (12) and (13).

$$G_{th} = \frac{\left(\frac{A_{th}^{\infty}}{N_T}\right)^{Au}}{\left(\frac{A_{th}^{\infty}}{N_T}\right)^{Au-Al}} \tag{12}$$

$$G_{ep} = \frac{\left(\frac{A_{ep}^{\infty}}{N_T}\right)^{Au}}{\left(\frac{A_{ep}^{\infty}}{N_T}\right)^{Au-Al}} \tag{13}$$

The epithermal neutron flux is defined by equation (14),

$$\varphi_{\text{ep}} = \frac{A_{cd}^{\infty}}{N_T . I_R^{\infty} . G_{ep}} . \ln \frac{E_2}{E_{cd}} \tag{14}$$

where:
I_R^{∞} is known as resonance integral and is treated in literature between the limits E_{Cd} and E_2, which refer to the cutting energy of cadmium and the edge of the intermediate region and the region of the fast neutronic spectrum [2];
N_T is the number of target nuclei;
G_{ep} disturbance factor in the epithermal flux.

4. RESULTS

The efficiency found for the HPGe detector in the position used for all counts of decay in the MAESTRO software was 0.009174 or 0.9174% with an error of 0.0002 or 0.0218%. The gamma branching rate of the ^{198}Au used was 0.9556 [2].

The correction disturbance factors for thermal neutron flux (G_{th}) and epithermal (G_{ep}) found experimentally are respectively 0.887 and 0.5821.

The cadmium-correction factor (Fcd) used was calculated using the MCNP software and equation 8, it is 1.054 ± 0.021 for infinitely dilute gold-foils and 1.098 ± 0.022 for high purity gold-foils.

The tables below show the neutron flux values for the regions corresponding to lucite board in various positions in the reactor core.

2013 International Nuclear Atlantic Conference - INAC 2013
Recife. PE. Brazil. November 24-29. 2013
ASSOCIAÇÃO BRASILEIRA DE ENERGIA NUCLEAR - ABEN
***ISBN:* 978-85-99141-05-2**

Table 1: Neutron flux in the channel 14-15.

Foil*	Thermal Flux(N/cm^2.s)	Error (%)	Epithermal Flux(N/cm^2.s)	Error(%)
637A	1.4051E+08	6.21	2.0643E+08	2.07
637B	2.2386E+08	7.94	3.5622E+08	2.70
637C	3.8054E+08	5.85	3.5413E+08	2.73
637D	3.2869E+08	4.23	2.6555E+08	2.54
637E	3.1305E+08	3.27	8.3862E+07	4.06
546A	8.5414E+07	3.95	4.7936E+08	3.66
546B	3.9697E+08	8.05	7.8771E+08	2.13
546C	6.0846E+08	6.99	8.2892E+08	2.43
546D	6.0483E+08	5.80	6.3089E+08	2.67
546E	4.9748E+08	3.71	2.0950E+08	3.15
455A	1.1178E+08	2.59	6.9747E+08	2.24
455B	4.9781E+08	11.29	1.1925E+09	2.45
455C	7.9669E+08	7.04	1.1834E+09	2.36
455D	8.8607E+08	4.69	9.1891E+08	2.08
455E	6.9111E+08	3.29	3.2995E+08	3.48
364A	1.2959E+08	2.57	8.1015E+08	2.21
364C	8.2240E+08	6.36	1.3643E+09	1.90
364D	9.6768E+08	5.94	1.0393E+09	2.78
364E	7.2310E+08	3.70	3.9005E+08	3.38
273A	1.3603E+08	3.02	7.2375E+08	3.05
273B	4.7171E+08	11.40	1.2439E+09	2.23
273C	6.3742E+08	11.68	1.3238E+09	2.72
273D	8.1734E+08	5.40	9.7986E+08	2.23
273E	6.1426E+08	6.76	3.8972E+08	6.05
182A	1.1015E+08	2.09	5.3088E+08	2.29
182B	3.2468E+08	1.32	9.6223E+08	2.39
182C	5.7593E+08	7.45	9.7824E+08	2.33
182D	5.7540E+08	5.48	7.4881E+08	2.04
182E	4.2289E+08	4.48	3.0564E+08	2.58
91A	1.3028E+08	1.31	2.6430E+08	3.65
91B	2.5594E+08	9.02	4.6645E+08	2.71
91C	3.9316E+08	6.25	4.9749E+08	2.45
91D	3.9924E+08	4.70	3.7381E+08	2.48
91E	3.0809E+08	3.22	1.4876E+08	3.21

***** Positions A. B. C and D correspond to the radial poin

**** Neutron flux at central position in the reactor core**

***** Maximum Thermal neutron flux in the reactor core.**

***ISBN:* 978-85-99141-05-2**

Table 2: Neutron flux in the channel 10-11.

Foil*	Thermal Flux(N/cm^2.s)	Error (%)	Epithermal Flux(N/cm^2.s)	Error(%)
637A	3.5375E+08	1.57	1,1922E+08	2.12
637B	5.2075E+08	2.22	3,3569E+08	1.97
637C	3.9287E+08	3.34	4,3151E+08	1.96
637D	1.5639E+08	5.81	3,2220E+08	1.92
637E	2.2267E+08	2.99	2.0732E+08	2.14
546A	5.3865E+08	4.40	2.9403E+08	4.40
546B	7.1064E+08	3.38	7.8457E+08	2.03
546C	6.4041E+08	4.87	1.0201E+09	2.10
546D	4.9964E+08	5.38	9.0844E+08	2.03
546E	3.3868E+08	4.96	5.2022E+08	2.25
455A	7.5890E+08	2.09	4.5281E+08	1.95
455B	9.7915E+08	4.06	1.1767E+09	2.26
455C	8.7350E+08	5.14	1.4781E+09	2.09
455D	7.3509E+08	5.62	1.3990E+09	2.03
455E	4.8479E+08	4.81	7.7636E+08	2.05
364A	8.1757E+08	2.16	5.2676E+08	1.91
364B	1.0583E+09	3.86	1.3314E+09	2.02
364C	9.5845E+08	4.81	1.6240E+09	1.90
364D	7.2759E+08	6.80	1.5084E+09	2.37
364E	5.7474E+08	4.26	8.2890E+08	1.96
273A	7.3696E+08	2.46	5.3403E+08	2.09
273B	9.1375E+08	4.21	1.2395E+09	2.19
273C	8.6821E+08	5.40	1.5677E+09	2.06
273D	7.0853E+08	6.14	1.4511E+09	2.10
273E	5.3123E+08	4.39	7.9608E+08	1.95
182A	4.9840E+08	2.53	3.9141E+08	1.96
182B	6.6237E+08	4.34	9.3407E+08	2.06
182C	6.0072E+08	5.88	1.2394E+09	1.97
182D	5.0169E+08	6.19	1.0600E+09	2.05
182E	3.5403E+08	4.78	5.6432E+08	2.03
91A	3.4232E+08	2.16	2.0856E+08	2.11
91B	4.6095E+08	3.29	5.0043E+08	1.94
91C	4.9240E+08	3.93	6.4775E+08	1.97
91D	3.9763E+08	4.35	5.8527E+08	2.01
91E	2.6737E+08	3.71	3.0567E+08	2.27

***** Positions A,B, C and D correspond to the radial points.

***ISBN:* 978-85-99141-05-2**

Table 3: Neutron flux in the channel 06-07.

Foil*	Thermal Flux($N/cm^2.s$)	Error (%)	Epithermal Flux($N/cm^2.s$)	Error (%)
637A	3.0591E+08	3.61	3.0672E+08	2.54
637B	2.5264E+08	4.25	3.4719E+08	2.07
637C	1.2810E+08	5.21	2.3228E+08	1.96
546A	4.0901E+08	2.93	3.6988E+08	2.01
546B	3.9047E+08	5.89	8.0661E+08	1.95
546C	3.6795E+08	4.97	6.4577E+08	1.90
455A	5.7963E+08	3.07	5.2473E+08	2.16
455B	5.6468E+08	6.04	1.1638E+09	2.12
455C	6.0842E+08	4.56	9.5651E+08	1.94
364A	6.3674E+08	3.00	5.8879E+08	2.07
364B	6.9039E+08	5.31	1.3044E+09	1.89
364C	7.2555E+08	4.58	1.0659E+09	2.14
273A	6.0850E+08	3.00	5.4816E+08	2.08
273B	6.1180E+08	5.88	1.1880E+09	2.22
273C	6.5126E+08	4.68	1.0158E+09	2.03
182A	4.4484E+08	2.84	3.9593E+08	2.03
182B	4.4303E+08	5.95	8.5754E+08	2.17
182C	4.7878E+08	4.42	7.3643E+08	1.91
91A	3.5855E+08	2.94	3.3951E+08	1.94
91B	3.7398E+08	3.37	4.1244E+08	1.97
91C	3.5769E+08	3.35	3.5032E+08	2.29

*Positions A,B, C and D correspond to the radial points.

Table 4: Neutron flux in the channel 02-03.

Foil*	Thermal Flux($N/cm^2.s$)	Error (%)	Epithermal Flux($N/cm^2.s$)	Error (%)
637C	2.0753E+08	3.48	2.4409E+08	1.91
546C	2.2749E+08	7.30	5.5454E+08	2.15
455C	3.1606E+08	6,37	7.1060E+08	1.95
364C	3.9604E+08	6.14	8.7325E+08	1,89
273C	3.3645E+08	6.44	7.7139E+08	1.93
182C	2.4294E+08	6.46	5.6279E+08	1.91
91C	2.5180E+08	3.57	3.0471E+08	1.90

* Positions A, B,C and D correspond to the radial points.

The graphs in the figures below show the curves of the neutron flux at various positions of the reactor core IPEN/MB-01.

2013 International Nuclear Atlantic Conference - INAC 2013
Recife. PE. Brazil. November 24-29. 2013
ASSOCIAÇÃO BRASILEIRA DE ENERGIA NUCLEAR - ABEN
***ISBN:* 978-85-99141-05-2**

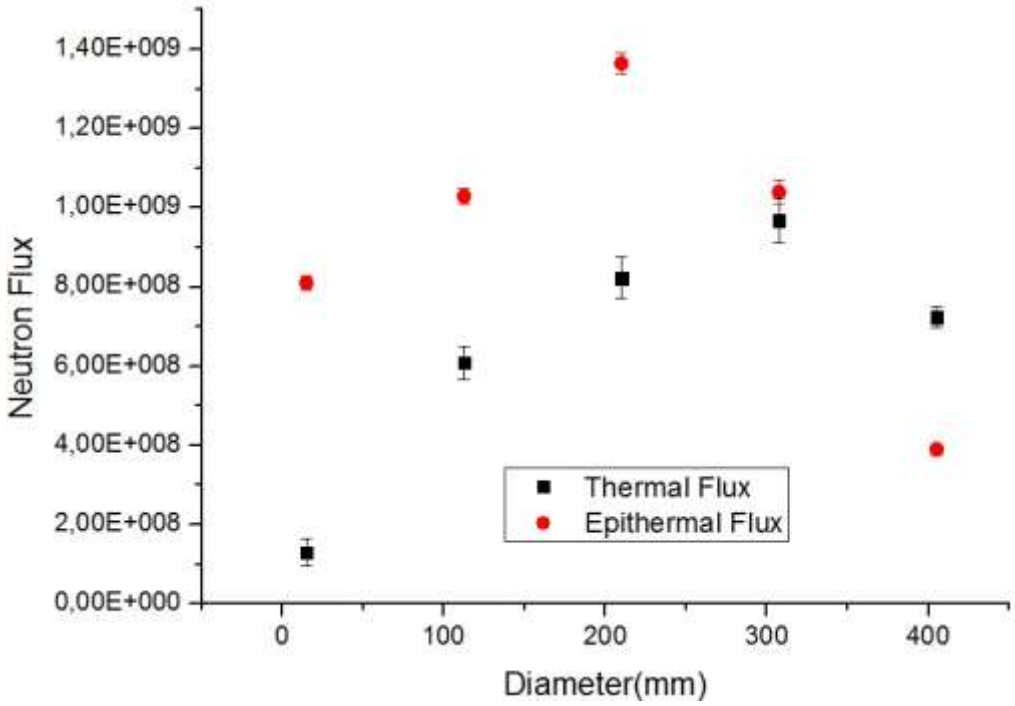

Figure 1: Curve of the neutrons flux at the radial east-west position in the center of the reactor core.

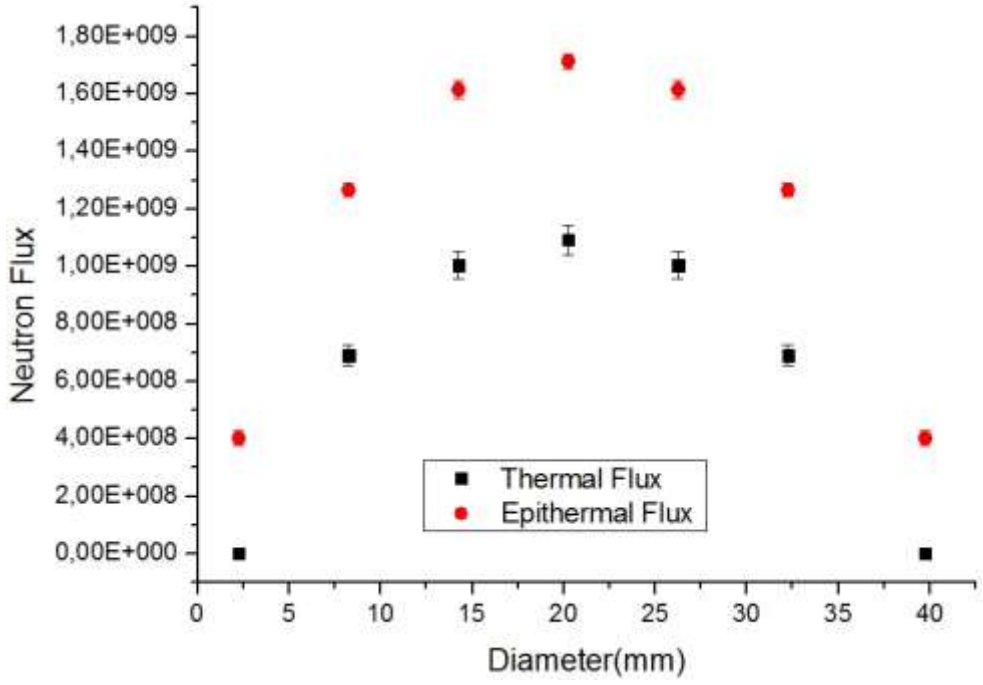

Figure 2: Curve of the neutrons flux at the radial north-south position in the center of the reactor core.

***ISBN:* 978-85-99141-05-2**

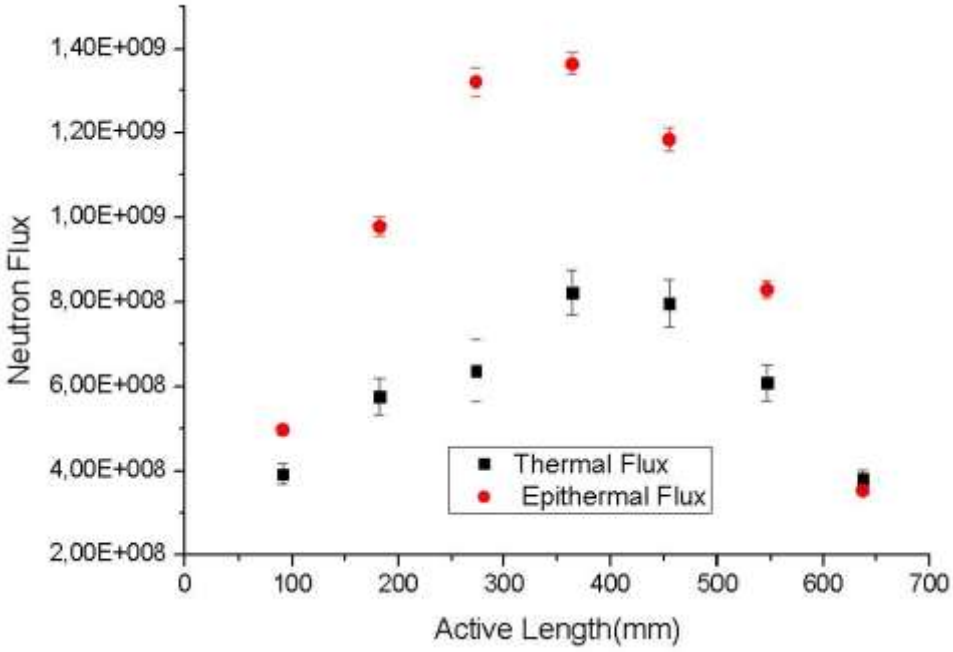

Figure 3: Curve of the axial neutrons flux in the center of the reactor core.

The neutron spectrum energy was obtained trough the code SANDBP with experimental data. Table 5 shows the neutron fluxes in various energy ranges in the center of the reactor core. Figure 4 shows the neutron spectrum energy in the center of the reactor core obtained by SANDBP code in IPEN/MB-01 reactor with the experimental results of saturation activity.

Table 5: Neutron Flux Obtained by SANDBP Code in the Central Position of the Reactor Core.

Energy (MeV)	Integral Neutron flux (n/cm^2s)
$>1.10^{-10}$	$5.1175.10^9$
$< 0.20.10^{-6}$	$8.2773.10^8$
$< 0.56.10^{-6}$	$9.7167.10^8$
> 0.1	$2.4757.10^9$
>0.4	$2.0093.10^9$
>0.5	$1.9064.10^9$
>1.0	$1.3938.10^9$

***ISBN:* 978-85-99141-05-2**

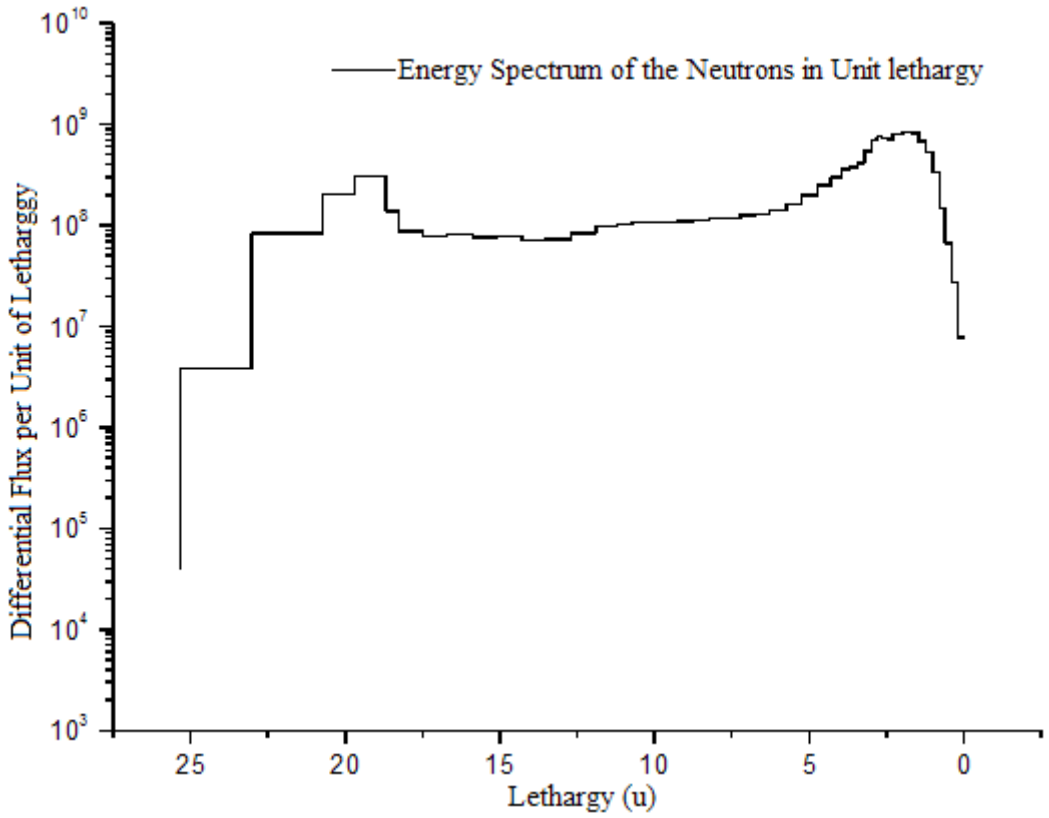

Figure 4: Neutron Spectrum Energy in the center of the Reactor IPEN/MB-01 in 50 Groups in Units Lethargy.

5. CONCLUSIONS

This work presents the experimental methodology for analysis of spatial and energy characteristics of the thermal and epithermal neutron flux in the reactor IPEN/MB-01. For this, we used the technique of activation analysis from the radiation of activation detectors foil type positioned along 4 irradiation channels in one hemisphere of the reactor core IPEN/MB-01. The symmetry condition of this reactor allows application of the results obtained for the other hemisphere.

The value found for the neutron flux satisfies the expectations, since the higher flux values are located in the center of the reactor core.

The minor excess of reactivity of this cylindrical configuration decreased the disturbance caused by the control rods in the values of neutron flux. The control rods were almost completely removed, and the values for the neutron flux in the upper part of the reactor core approached to the value of the bottom, away from disturbance of control rods.

The real operating power measured by activation technique was obtained using the experimental neutron flux presented in this work and too the measure of the curvature of leakage "Buckling" using the experimental data of this work [11]. The value of the power level to cylindrical configuration obtained was (92.08±0.07) watts [10].

***ISBN:* 978-85-99141-05-2**

For the neutron spectrum, it is suggested that radiate detectors operate in the range 100 keV to 1 MeV; should be used as detectors preferred alloys infinitely diluted in order to avoid the effects of disturbance of the flux.

ACKNOWLEDGMENTS

Acknowledge the help of colleagues Flávio Betti, Rogério Jerez, Luíz Ernesto and Hugo Landim, and the sources of funding of the CNEN.

REFERENCES

1. Profio, A.E. *Experimental Reactor Physics*. New York, Wiley, 1976.
2. Bitelli, Ulysses d' Utra. "Medida e Cálculo da Distribuição Espacial e Energética de Nêutrons no Núcleo do Reator IEA-R1". Dissertação de mestrado,IPEN, 1988.
3. Suich,J.E; Honeck, H.C. *The Hammer System Heterogeneous Analysis of Multigroup Methods of Exponential and Reactor*. Aiken,S.C., Du Pont de Nemours, Savannah River Laboratory, 1967 (DP-1064);
4. Westcott, C.M. Effective Cross Section Values for Well-Moderated Thermal Reactor Spectra. Clalk River, Ontário, Atomic Energy of Canada, Sep. 1960 (AECL-1101).
5. Harmon, C.D., Busch, R.D., Briesmeister, J.F., Forster, R.A. Criticality Calculations with MCNP: A Primer**.** Los Alamos National Laboratory, LA-12827-M Manual, 1994.
6. Beckurtz, K.H.;Wirtz, K. Neutron physics**.** New York, Springer, 1964.
7. Bench, F. ; Fleck,C.M. Prática de Física de Nêutrons - Volume 2, Tradução DERE/IEN , pág.306 .
8. Zjolnay,E.M. Neutron Flux and Spectrum Measurement by Activation Method. Lectures Notes for the Training Course and Measurements of Neutron Flux Spectrum for Research Reactor, IAEA, Serpong, Hacarta, Indonesia, 27 september-15 October,1993.
9. Bardos, J.; Becker, R.; Dabronski, C.; Gacsi, L.; Gadó, J.; A.; SZATMÁRY, Z.; et alli.. *Experimental Investigations of the Physical Properties of WWER-Type Uranium-Water Lattices*. In: FINAL REPORT OF TEMPORARY INTERNATIONAL COLLECTIVE. Budapest, Akadémiai Kiadó, VOLUME 1, 1985.
10. Bitelli, U.d'Utra, da Silva, A.F.P, Mura, L.E.C., Arêdes, V.O.G., dos Santos, D.F., "Calibration of the nuclear power channels for the Cylindrical configuration of the ipen/mb- 01 reactor obtained from the measurements of the spatial Neutron flux distribution in the reactor core through the irradiation of gold foils", International Nuclear Atlantic Conference , Recife, PE, Brazil, 24-29 November, 2013.
11. Purgato R.T, Bitelli U.d´Utra, Arêdes V.O, da Silva A.F.P, dos Santos D.F, Mura L.F.L and Jerez R., "Determination of Buckling in the IPEN/MB-01 Reactor in Cylindrical Configuration" , International Nuclear Atlantic Conference , Recife, PE, Brazil, 24-29 November, 2013.